

Classification of Planck catalog of SZ sources and their energy spectral distribution

Thibault Barnouin

Kewen Zhang

03/26/2021

Abstract

In this report we use the second Planck catalog of Sunyaev-Zel'dovich sources (PSZ2) to build three samples distinguishing high-reliability clusters, known clusters and candidate clusters. We stacked these three samples at different frequency of Planck full sky map, we observed a distinct disappearing signature of known clusters and high-reliability clusters due to the Sunyaev-Zel'dovich effect at 217GHz. We then compute the flux of each sample at different frequency. Having the spectral energy distribution of each sample, we fit them with the SED law of SZ effect, thermal dust contamination and combined effect of these two. These plots also confirm that for known clusters and high-reliability clusters the SZ effect is dominant, but they are significantly affected by the thermal dust in the IR domain, and the candidate clusters are highly dominated by thermal dust contamination.

1 Introduction

1.1 Cosmic microwave background and Planck mission

When the temperature of the universe drops to $T \approx 3000K$, the nuclei and electrons are combined under electromagnetic interaction, the matter content in the universe is starting to transform from ionization state (plasma) to neutral state rapidly. When at the ionization state, photons frequently interacts with charged particles (eg. by Compton scattering). Charged particles are in thermal equilibrium with matter, whereas photon hardly interacts in neutral state. Thus after the combining of charged particles into neutral atoms, the universe starts to become transparent. Before photon decoupling, photons and matter were in thermal equilibrium, which energy density is similar to the black body radiation described as $du = \frac{8\pi hc}{\lambda^5} (\exp \frac{hc}{kT\lambda} - 1)^{-1} d\lambda$, where du is the unit cubic energy in wavelength ($\lambda, \lambda + d\lambda$), T is temperature, c is speed of light, h and k are Planck and Boltzmann constant. After decoupling the energy spectrum of photon still satisfies Planck equation, but rescales with scale factor a , $T' = a^{-1}T$. The temperature of decoupled photon today is $T_{CMB} \approx 2.7255K$, whose energy is concentrated at microwave band. We are immersed in a background of photons whose energy density is described by the blackbody radiation curve of T_{CMB} according to the wavelength distribution, this is called Cosmic Microwave Background (CMB).

From previous cosmic microwave background experiments, we know that there are anisotropies in CMB, $T_1/T_0 \sim 10^{-3}$ and $T_2/T_0 \sim 10^{-5}$. Planck is a space telescope designed to measure CMB anisotropies with high precision and CMB related universe structures.

1.2 Sunyaev-Zel'dovich effect

One of the important effect on CMB photons that can be measured by Planck is the Sunyaev-Zel'dovich (SZ) effect. This effect is the distortion of the CMB through inverse Compton scattering by high-energy electrons in galaxy clusters, resulting a boost in CMB photons. The SZ effect can be divided into thermal and kinematic effects - thermal effects being CMB photons interacting with electrons that have high energies due to their temperature, and kinematic effects being a second-order effect due to the bulk motion of high energy electrons. Here we only consider thermal SZ effects in non-relativistic regime. The thermal SZ effect introduce secondary CMB temperature fluctuations:

$$\Delta I_{SZ} = yf(x)I_0 \quad (1)$$

where $x = h\nu/k_B T_{CMB}$, $I_0 = 2(k_B T_C MB)^3/(hc)^2$, $f(x)$ is the frequency dependence:

$$f(x) = \frac{x^4 e^x}{(e^x - 1)^2} \left(x \frac{(e^x + 1)}{(e^x - 1)} - 4 \right) \quad (2)$$

y is Compton y parameter:

$$y = \int n_e \frac{k_B T_e}{m_e c^2} \sigma_T dl \quad (3)$$

where n_e is electron number density, T_e is the electron temperature, $m_e c^2$ is the electron rest mass energy, and the integration is along the line of sight. In non-relativistic limit, the spectral shapes only depend on x . The frequency dependence gives a unique way to detect clusters. (1)

2 Data analysis and results

We use the Planck full sky maps at frequencies of 100, 143, 217, 353, 545 and 857 GHz combined with PSZ2 to analysis the spectral energy distribution.

2.1 Clusters classification

We present in this paper 3 different samples from the PSZ2 catalog to distinguish high-reliability clusters, known clusters and candidate clusters.

We first choose the redshift as a signature to distinguish known clusters and candidate clusters. Known clusters are validated by other experiments and their redshift have been measured whereas candidates have not been validated. The second criterion we consider is Q_{Neural} to select high-reliability clusters. It is deduced from a neural network trained on confirmed clusters in the PSZ1, clusters in radio, IR and X-ray catalogs and random positions on the sky. This gives us $Q_{Neural} = 0.4$ as the threshold for low-reliability detection (2), so we take this to classify highly-reliability clusters.

And at infrared region, there is a high contamination from thermal dust, this effect is given by:

$$s_d = A_d \left(\frac{\nu}{\nu_0} \right)^{\beta_d + 1} \frac{e^{\gamma \nu_0} - 1}{e^{\gamma \nu} - 1} \quad (4)$$

where A_d , β_d and T_d are free parameters of the model, $\gamma = \frac{h}{k_B T_d}$, $\nu_0 = 545\text{GHz}$ [(4)].

2.2 Stacking clusters at different frequencies

From PSZ2 we can acquire the galactic coordinates of each potential cluster, we make the 2D map of these potential clusters from the Planck full sky map, stacking them into one map to average the background under the assumption that the are all point sources.

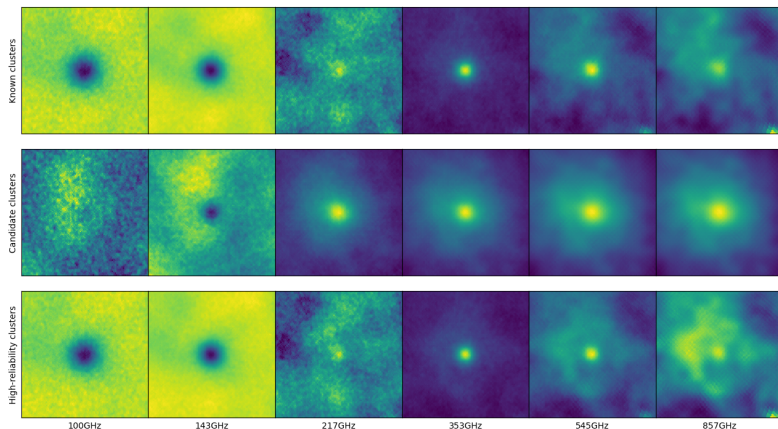


Figure 1: Stacked signal in six Planck frequencies(100GHz to 857GHz from left to right column). From upper to lower row are the three samples we extract from PSZ2, known clusters , candidate clusters, and high-reliability clusters

2.3 Spectral energy distribution

We obtain the flux in stacked map using aperture photometry at each frequency of Planck full sky map. We assume the cluster is a point source for our detector and select an aperture angle equal to the FWHM of the 143GHz channel. We are then able to compute a value of the integrated flux of the cluster without its background. We do so for our three sample and their SED can be seen in Figures 2, 3 and 4.

On this SED we fit a model that take into account both contributions from thermal dust (see eq (4)) and SZ effect given by the following :

$$s_{sz} = y_{sz} \cdot f(x) \quad (5)$$

Where y_{sz} is a free parameter of the model and $f(x)$ is defined in eq (2).

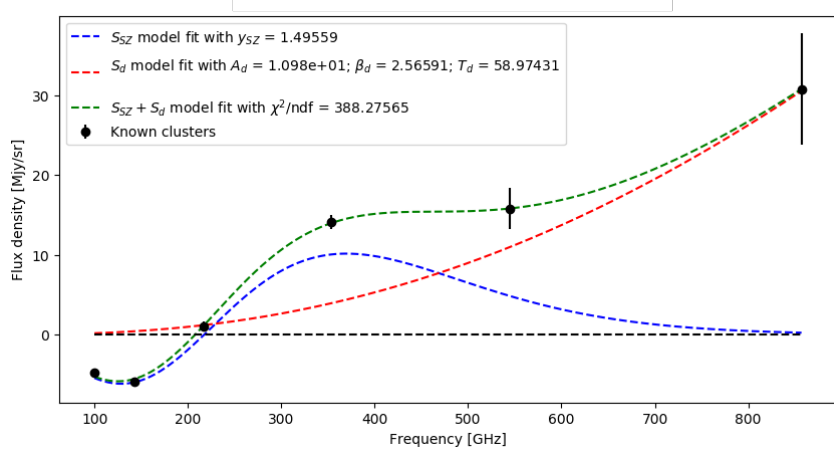


Figure 2: SED of the SZ effect for known clusters

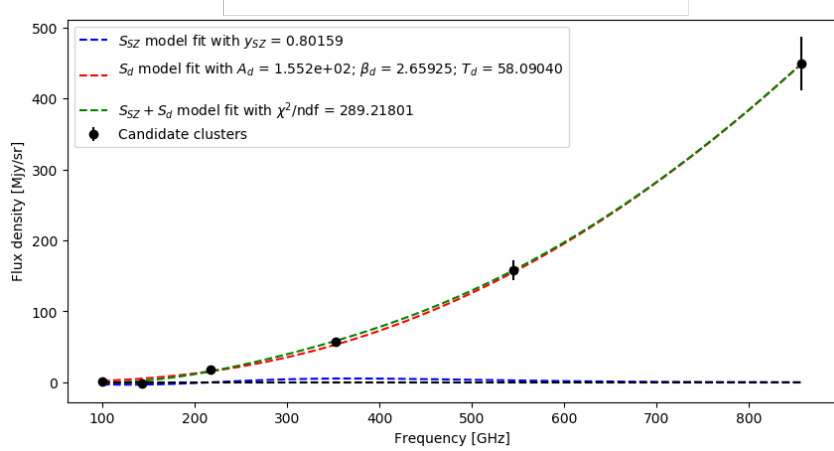


Figure 3: SED of the SZ effect for candidate clusters

3 Discussion

During this project we reproduced the SZ cluster validation from the Planck 2013 results paper (3) by looking at the SZ effect in the full sky map given a catalog of objects. To estimate the errors on our results we used the 'bootstrap' technic. This technic give us a range of flux values for the stacking of a given object sample. We then get high relative errors for low statistics sample and at high frequencies due to IR contamination from inter-stellar medium dust. Our χ^2 values are high due to small errors at low frequencies, which may be due to under-estimated errors.

Given these three samples we were able to see that our analysis code allows us to see relative contribution from SZ effect and Thermal dust in the observation of the CMB.

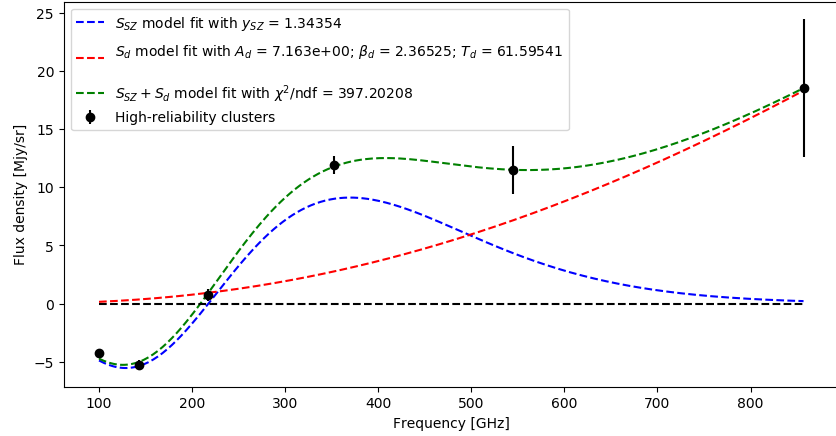


Figure 4: SED of the SZ effect for High-reliability clusters

References

- [1] Carlstrom J E, Holder G P, Reese E D. Cosmology with the Sunyaev-Zel'dovich effect[J]. Annual Review of Astronomy and Astrophysics, 2002, 40(1): 643-680.
- [2] Aghanim N, Hurier G, Diego J M, et al. The Good, the Bad, and the Ugly: Statistical quality assessment of SZ detections[J]. Astronomy Astrophysics, 2015, 580: A138.
- [3] Planck Collaboration, Planck 2013 results. XXIX. The Planck catalogue of Sunyaev-Zeldovich sources, Astronomy Astrophysics, 2014, <http://dx.doi.org/10.1051/0004-6361/201321523>
- [4] Planck Collaboration, Planck 2015 results. X. Diffuse component separation: Foreground maps, Astronomy Astrophysics, 2016, <http://dx.doi.org/10.1051/0004-6361/201525967>